Hindawi Publishing Corporation
Science and Technology of Nuclear Installations
Volume 2016, Article ID 5852328, 6 pages
http://dx.doi.org/10.1155/2016/5852328

Research Article

Development of a Composite Technique for Preconditioning of 41Cr4 Steel Used as Gear Material: Examination of Its Microstructural Characteristics and Properties

Jianjun Hu,[1,2] Chaoping Ma,[1] Hongbin Xu,[2] Ning Guo,[3] and Tianfeng Hou[1]

[1]*College of Material Science and Engineering, Chongqing University of Technology, Chongqing 400054, China*
[2]*Chongqing Municipal Key Laboratory of Institutions of Higher Education for Mould Technology, Chongqing 400054, China*
[3]*Faculty of Materials and Energy, Southwest University, Chongqing 400715, China*

Correspondence should be addressed to Hongbin Xu; kbe@vip.cqut.edu.cn and Ning Guo; guoning_1000@163.com

Received 22 May 2016; Revised 23 July 2016; Accepted 10 August 2016

Academic Editor: Parashuram Sahoo

Commercial 41Cr4 (ISO standard) steel was treated by a composite technique. An intermediate layer was introduced firstly at the 41Cr4 steel surface by traditional carburizing and nitriding. Then a hard Cr coating was brush-plated on the intermediate layer. Finally, the coating layer was modified by high current pulsed electron beam (HCPEB), followed by quenching and subsequent tempering treatment. The microstructure, mechanical properties, and fracture behavior were characterized. The results show that a nanocrystalline Cr coating is formed at the 41Cr4 steel surface by the treatment of the new composite technique. Such nanocrystalline Cr coating has acceptable hardness and high corrosion resistance performance, which satisfies the demands of the gears working under high speed and corrosive environment. The composite process proposed in this study is considered as a new prospect method due to the multifunction layer design on the gear surface.

1. Introduction

Gear is a vital device in the gear transmission system which can transmit power, change the direction and speed of movements, and influence the performance of the whole equipment [1]. With the progress of technology and the development of gear transmission, the gear is developed towards high speed, heavy load, complex service environment, and high reliability. Moreover, more strict requirements such as large gear ratio, efficiency transmission, and lightweight are necessities for the gears used in aviation, aerospace, and navigation fields [2–4]. However, it is difficult to achieve those goals through increasing modulus or thickness of the gears. Instead, the applications and developments of surface treatment techniques for improving the strength of the gear tooth face are considered as a potentially effective approach.

Traditionally, tooth face strengthening methods, such as carburizing, nitriding, surface and quenching, have been applied singly to harden the gears. It has been reported that both surface hardness and wear resistance can be improved by the application of single traditional method [5–9]. Modern gears often work under complex circumstance, such as high speed, high temperature, and highly corrosive environment, which results in a multifunction of the gear surface. However, such multifunction gear cannot be obtained by singly using traditional methods. It has been reported that coating with Cr layers on the materials is an important engineering practice to improve the corrosion resistance. High current pulsed electron beam (HCPEB) treatment has been reported as an effective way for strengthening the bonding force between coating layer and substrate [10]. Thus, in this work, a composite process has been developed to treat 41Cr4 steel which is widely used as gear materials. Microstructures, mechanical properties, and fracture behavior of the 41Cr4 steel treated by the new composite process have been characterized and discussed.

2. Experimental Section

Commercial 41Cr4 steel (0.40% C, 0.8% Cr, Ni ≤ 0.30%, 0.23% Si, and 0.7% Mn in wt.) was chosen as the original materials in this study. Conventional carburizing and nitriding treatments have been carried out firstly in order to introduce an intermediate layer on the surface of the original materials. Brush-plating was performed on the intermediate layer to obtain Cr coating after carburizing and nitriding processes. A direct current power pack (MBPK-50A) was performed with a voltage of 10 V. HCPEB (RITM-2M type) treatment with a voltage of 27 KV and a pulse number of 35 was carried out followed by subsequent quenching at 850°C and tempering at 250°C for 25 minutes, respectively.

Microstructures were observed with a metallographic microscope (Carl Zeiss A10), a super depth filed microscopy (Kean VR-3000), and a field emission gun scanning electron microscope (FEG-SEM, Zeiss Sigma HD). Both secondary electron imaging (SEI) and back-scattered electron imaging (BSEI) techniques were carried out for the characterization of the microstructure. The composition distribution along the depth direction of the gear surface was analyzed by the energy dispersive spectrometer (EDS) equipped in the FEG-SEM. Microhardness along the depth direction was tested by a hardness tester (HVS-1000) with a load of 0.5 N and a loading time of 10 s. The reciprocating dry sliding was carried out on a ball-on-flat tribometer (HSR-2M). The friction pair was Si_3N_4 ceramic ball (hardness 1800 HV) with a diameter of 6 mm. The corrosion resistance performance was carried out on a PAR273A constant potential instrument. Potentiodynamic polarization potential ranged from −0.1 to 0.5 V.

3. Results and Discussion

3.1. Microstructure. Surface microstructures of Cr coating prepared by brush-plating before and after HCPEB treatment are illustrated in Figures 1(a) and 1(b), respectively. It can be seen that, before HCPEB, the Cr coating shows morphology of nonuniform equiaxed nodular units (the average size is 26 μm in diameter), rather than polycrystalline structures. Such morphology resulted by the combined action of continuous supply of plating solution, contact pressure, and speed between anode and cathode [11–14]. In contrast, after HCPEB treatment, the surface of the Cr coating is more smooth, and all the small equiaxed nodular units almost disappear, which results in a uniform distribution of equiaxed nodular units (the average size is 46 μm in diameter,) within the Cr coating (see Figure 1(b)). However, as shown in Figure 1(b), there are some small cracks and erupted craters existing within the Cr coating, suggesting that rapid melting and cooling have taken place during the HCPEB treatment. Cracks within the coating are considered as the results of residual thermal stress which are formed due to the rapid cooling rates of HCPEB. It has been reported that internal tensile stress is existing in deposited nickel-tungsten alloy coating, which results in same small cracks within the coating [15]. When the brush-plated Cr is irradiated with HCPEB, high energy electron beam is deposited on the Cr coating. Figure 1(b) indicates that the equiaxed nodular units form during brush-plating and regrow into nodular shape again during HCPEB treatment. It is more important that the uniform microstructure has been obtained by the effect of such melting and regrowth of Cr coating during HCPEB treatment.

Figure 2 shows the sectional view images of the sample surface after quenching and tempering. From Figure 2(a), it can be seen that the thickness of the Cr coating is about 112 μm and there are some cracks existing in the Cr coating. Both Cr and Fe distributions along the depth direction are determined by EDS line scanning, as shown in Figure 2(b). It shows clearly that a Cr layer has been coated on the 41Cr4 matrix. More Fe has been diffused into the Cr coating, while only a few of Cr exist in the 41Cr4 matrix. It indicates that Fe has a faster diffusion rate than Cr during the diffusion process. The sectional view images of the sample surface are also characterized by BSEI technique, as shown in Figure 3. It is well known that BSEI can display topography contrast, *Z*-contrast, and electron channeling contrast (ECC) information [16]. It can be seen that the 41Cr4 matrix has a pearlite microstructure (topography contrast), while the Cr coating has polycrystalline characteristics (ECC). The average grain size is determined as 260 nm (see Figure 2(d)). It is reported that, with quenching at 850°C followed by tempering at 250°C, the material surface is heated to cause recrystallization of Cr coating particles [11, 17]. It indicates that the crystallization behavior of the nodular shape particles of the Cr coating formed during HCPEB treatment has taken place during the subsequent quenching and tempering process.

Overall, a Cr coating composed by inhomogeneous nodular Cr particles is formed firstly after brush-plating. Then, such inhomogeneous structure is improved by the HCPEB treatment. Finally, the uniform nodular Cr particles are changed into polycrystalline structure with average grain size in nanoscale. That is, a nanocrystalline Cr coating is generated on the intermediate layer.

3.2. Microhardness. Figure 3 shows the sectional hardness plotted versus depth of the 41Cr4 steel treated by the new composite method. It can be seen that the microhardness of the 41Cr4 matrix is about 335 $HV_{0.5}$. And the microhardness of the sample after brush-plated Cr coating is about 932 $HV_{0.5}$. The section hardness of the sample after brush-plated Cr coating gradually decreased from the surface of 932 $HV_{0.5}$ to about 648 $HV_{0.5}$ at 880 μm and then eventually slightly increases to about 700 HV. In addition, no acute fluctuation is witnessed in the process of change. Moreover, it can be roughly estimated that the thickness of hard layer, the hardness of which is higher than 720 $HV_{0.5}$, is up to 280 μm. Therefore, it can be concluded that this process makes the hardness increase gradually from the core to material surface. And it also further illustrates that this process makes the performance of the gear section realize gradient change [18, 19].

3.3. Fracture Behavior. Artificial broken sample is used in the experimental process to further study the comprehensive

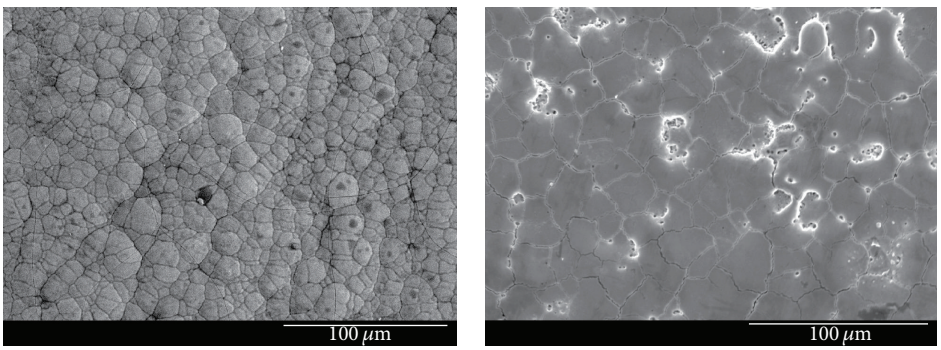

Figure 1: View of the surface morphology of Cr coating before (a) and after (b) HCPEB treatment. The images are obtained by SEI technique.

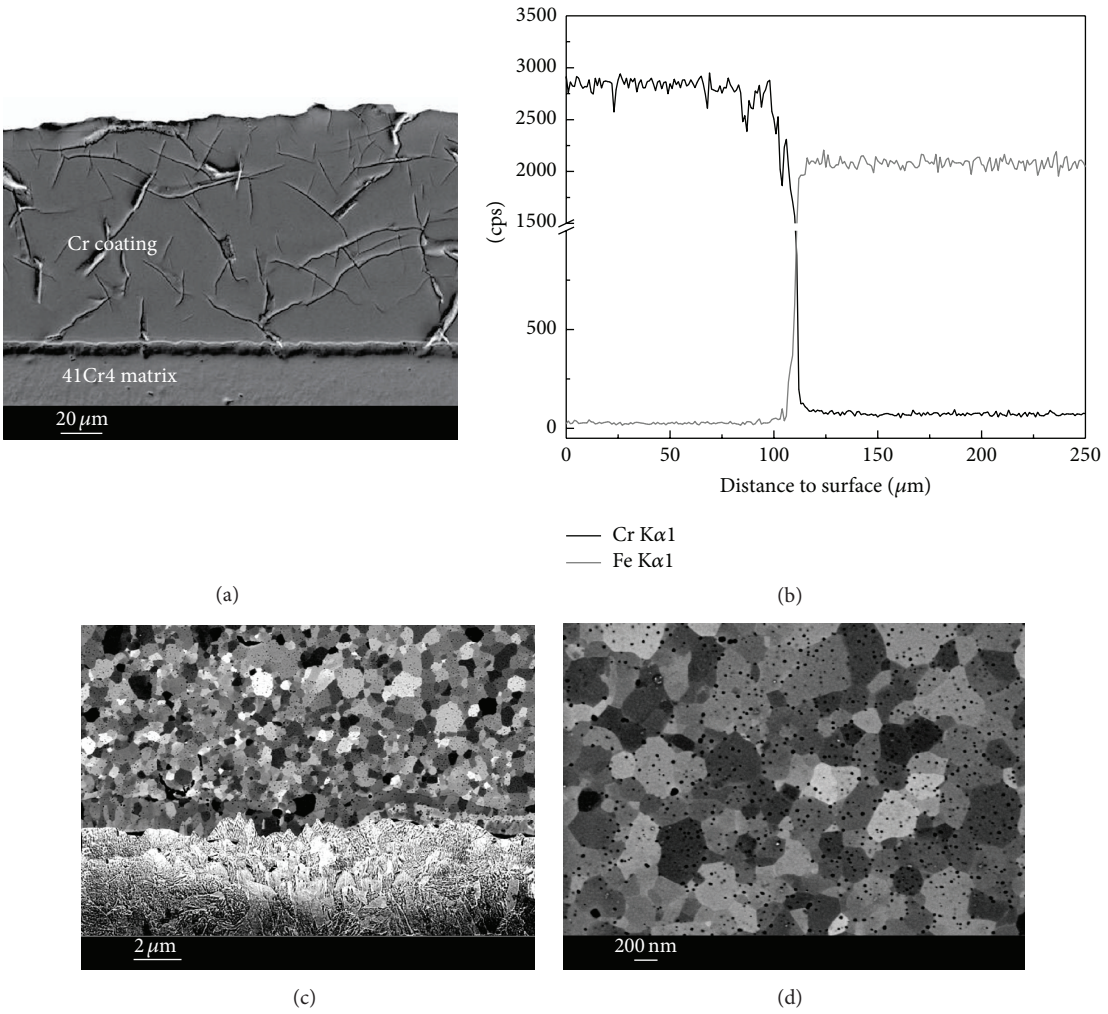

Figure 2: Sectional view of microstructure of the sample surface: (a) SEI image, (b) line scanning of EDS, (c) BSEI image, and (d) high magnification BSEI showing nanocrystalline Cr.

performance of the 41Cr4 steel treated by the composite process. The SEI technique is used to observe the fracture morphology from macro and micro perspectives, respectively, as shown in Figure 4.

The outer surface of the Cr coating is very flat in macro view, where a series of cleavage fracture appearances is observed (marked as Zone 1 in Figure 4(a)). Small stepped cleavage plane almost parallel to the direction of crack propagation can be seen in micro view, which is known as the river pattern fracture. Adjacent to the Cr coating, the fracture feature of the pearlite matrix (Zone 2 in Figure 4(a)) is revealed in Figure 4(c) and amplified in Figure 4(d). Clearly,

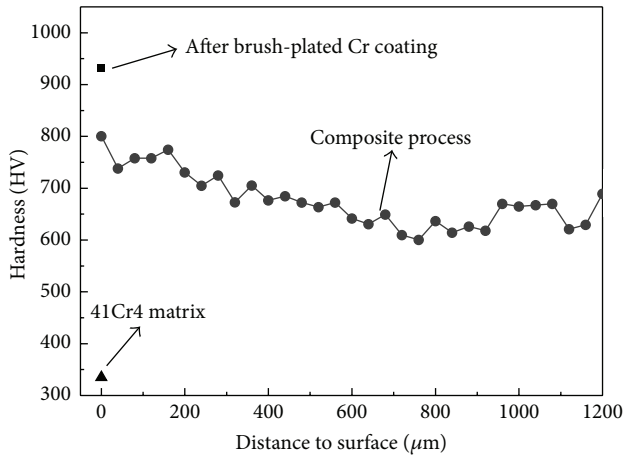

Figure 3: Microhardness plotted as a function of depth to the sample surface.

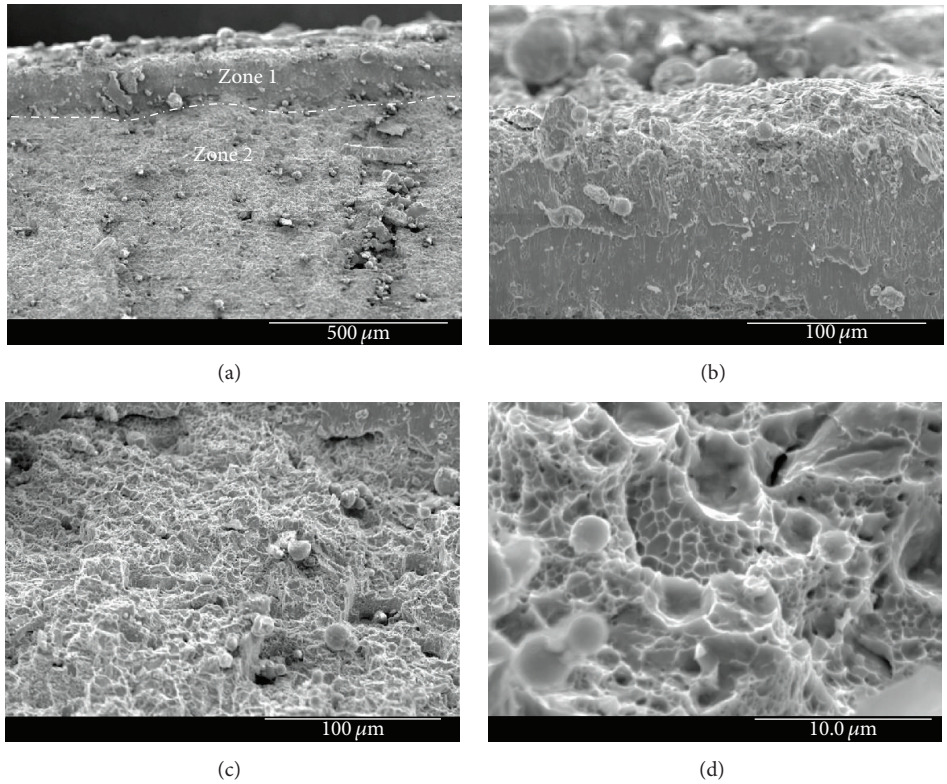

Figure 4: Fracture morphology of (a) the overall feature in (b) Zone 1 and in (c) Zone 2 and (d) high magnification of Zone 2.

many typical ductile dimples are observed in Zone 2, which indicates that the matrix has good plasticity. That is, the fracture morphology of the sample is gradually transformed from cleavage pattern in the coating to ductile dimple in the matrix. According to the micro mechanism of fracture, dimples are the results of microporous growth and often include inclusion or a second phase, which proves that the microvoids form at the interface between the inclusions or second phase and the substrate. The diameter and depth of dimples depend on the quantity distribution of the second phase and the plastic deformation ability of 41Cr4 matrix. Dimples are large and deep when the second phase is less and has uniform distribution, and the plastic deformation ability of substrate is strong as well. The dimples are large and shallow when the work hardening ability of substrate is very strong. Besides, the formation of the microvoids has two ways in this study: one is the fracture of interface which is between the substrate and the second phase particles and the other is the fracture induced by stress action between the two neighbor second phase particles. Under the internal

stress, the microvoids grow up gradually, which results in the final fracture during tensile test. Therefore, the fracture of the 41Cr4 matrix is ductile in this study.

For the samples treated by the composite technique, from surface to core, the fracture morphology shows a gradient change which evolves continuously from cleavages into ductile dimples. The river pattern fracture is observed in the sample surface because the crack grows along two adjacent paralleling cleavage planes with narrow spacing in the surface layer. Although the appearance of cleavage morphology generally implies brittle characteristics, it maintains relatively high hardness (see Figure 3) which is very important for high wear resistance. When moving towards the core of the sample, the tempered pearlite shows excellent toughness, and small microvoids gradually form in these places and grow into dimple during tensile test. It is concluded that high wear resistance and good toughness of 41Cr4 gear material have been realized via the new composite technique.

3.4. Friction Coefficient. Figure 5 shows the coefficient of friction of the 41Cr4 matrix and the sample with composite process. It can be seen that the friction coefficient of 41Cr4 matrix increases sharply into the maximum value of 0.22 during 0–0.7 min and then decreases gradually (0.7–2.3 min). However, after 2.3 min, it comes into a stable state with a mean friction coefficient of 0.17. For the sample with composite process, originally, the coefficient of friction has a rather higher value (about 1.55), and then it decreases into about 0.73 at 0.47 min. During 0.5–4.0 min, it suffers an increasing-decreasing-increasing change. After 4.0 min, it decreases into 0.78 gradually. This suggests that the coefficient of friction is very high at the beginning of contact due to the rough and hard material surface. However, it is still relatively low because the friction is still at the running stage and wears lightly. With increasing time, the friction coefficient starts to go up due to the micro convex body on the friction pair surface at the initial stage. With friction further developing, the ceramic ball is ground into a continually smoother surface, while the Cr coating is gradually oxidized and even generates wear debris. Thus, the original two-body friction converts into the three-body friction which greatly increases the wear rate. The friction coefficient decreases gradually with increasing time. Finally, the friction was developed into the stable wear stage.

3.5. Corrosion Resistance. The potentiodynamic polarization curves of the 41Cr4 matrix and sample with composite process are shown in Figure 6. Clear differences in the corrosion behavior of the two samples can be depicted. The sample of the 41Cr4 matrix has slightly larger corrosion current density (iccor) and lower corrosion potential (Eccor) than the sample with composite process. So, the corrosion resistance of 41Cr4 treated by carburizing and nitriding and then brush-plating Cr after treatment with electron beam was significantly improved compared with the 41Cr4 matrix [14, 20].

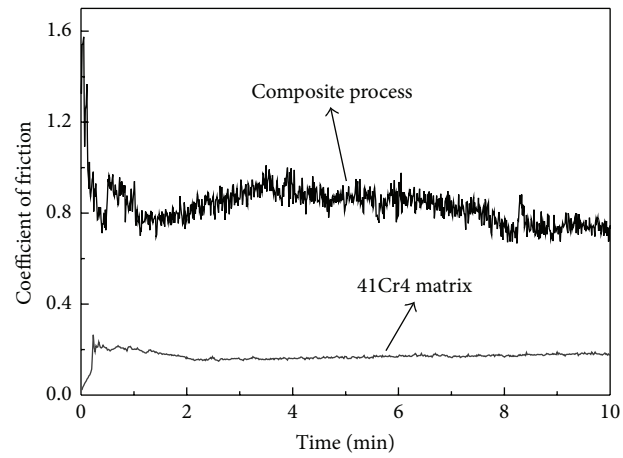

Figure 5: The friction coefficient plotted as a function of loading time.

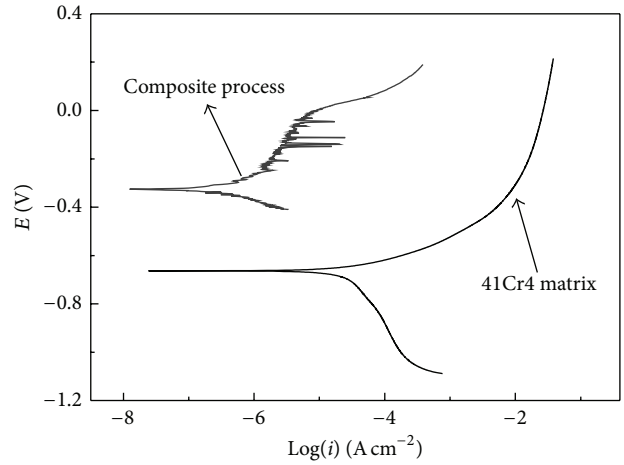

Figure 6: Polarization curve of 41Cr4 steel treated by the composite process.

4. Conclusions

Commercial 41Cr4 steel has been processed by a new composite process method in this study. Microstructure feature, mechanical properties, and fracture feature have also been characterized. Some conclusions can be drawn as follows:

(i) A nanocrystalline Cr coating layer is formed on the 41Cr4 steel surface after the treatment of the composite process.

(ii) The nonuniform microstructure of brush-plated Cr coating could be improved by remelting and regrowth behavior of Cr coating during HCPEB treatment.

(iii) The hardness increases gradually from core to surface of the 41Cr4 sample. The nanocrystalline Cr coating has acceptable hardness and is considered to have high corrosion resistance performance.

Competing Interests

The authors declare that they have no competing interests.

Acknowledgments

This study was supported by the National Natural Science Foundation of China (51275548 and 51575073), International Cooperation Special Project in Science and Technology of China (2015DFR70480), and Scientific and Technological Research Program of Chongqing (KJ1400902 and cstc2014gjhz70003).

References

[1] R. K. Pandey, "Failure analysis of coal pulveriser gear box," *Engineering Failure Analysis*, vol. 14, no. 4, pp. 541–547, 2007.

[2] H. C. Kim, "Sector gear and gas-insulated switchgear having the same," Patent US20130167675, 2013.

[3] G. Meschut, O. Hahn, D. Teutenberg, and L. Ernstberger, "Influence of the dosing and mixing technology on the property profile of two-component adhesives," *Welding in the World*, vol. 59, no. 1, pp. 91–96, 2015.

[4] V. Ngo, T. Hofman, M. Steinbuch, and A. Serrarens, "Effect of gear shift and engine start losses on energy management strategies for hybrid electric vehicles," *International Journal of Powertrains*, vol. 4, no. 2, pp. 141–162, 2015.

[5] X. Nie, "Study of the rapid surface modification technology," *Heat Treatment of Metals*, no. 3, pp. 19–22, 1997.

[6] M. Tarakci, K. Korkmaz, Y. Gencer, and M. Usta, "Plasma electrolytic surface carburizing and hardening of pure iron," *Surface & Coatings Technology*, vol. 199, no. 2-3, pp. 205–212, 2005.

[7] Z. J. Tian, L. I. Jie, D. J. Shen, and Y. L. Wang, "Liquid phase plasma electrolytic carburizing, nitriding, carbonitriding technique," *Electroplating & Finishing*, vol. 25, no. 2, pp. 53–56, 2006.

[8] C. Tsotsos, A. L. Yerokhin, A. D. Wilson, A. Leyland, and A. Matthews, "Tribological evaluation of AISI 304 stainless steel duplex treated by plasma electrolytic nitrocarburising and diamond-like carbon coating," *Wear*, vol. 253, no. 9-10, pp. 986–993, 2002.

[9] A. L. Yerokhin, A. Leyland, C. Tsotsos, A. D. Wilson, X. Nie, and A. Matthews, "Duplex surface treatments combining plasma electrolytic nitrocarburising and plasma-immersion ion-assisted deposition," *Surface & Coatings Technology*, vol. 142–144, no. 7, pp. 1129–1136, 2001.

[10] D. Wu, J. Zhang, J. C. Huang, H. Bei, and T. G. Nieh, "Grain-boundary strengthening in nanocrystalline chromium and the Hall-Petch coefficient of body-centered cubic metals," *Scripta Materialia*, vol. 68, no. 2, pp. 118–121, 2013.

[11] D. B. Bober, M. Kumar, and T. J. Rupert, "Nanocrystalline grain boundary engineering: increasing Σ3 boundary fraction in pure Ni with thermomechanical treatments," *Acta Materialia*, vol. 86, pp. 43–54, 2015.

[12] X. Bin-Shi, W. Hai-Dou, D. Shi-Yun, and J. Bin, "Fretting wear-resistance of Ni-base electro-brush plating coating reinforced by nano-alumina grains," *Materials Letters*, vol. 60, no. 5, pp. 710–713, 2006.

[13] B. Wu, B.-S. Xu, B. Zhang, X.-D. Jing, and C.-L. Liu, "Automatic brush plating: an update on brush plating," *Materials Letters*, vol. 60, no. 13-14, pp. 1673–1677, 2006.

[14] B. Subramanian, S. Mohan, and S. Jayakrishnan, "Structural, microstructural and corrosion properties of brush plated copper-tin alloy coatings," *Surface and Coatings Technology*, vol. 201, no. 3-4, pp. 1145–1151, 2006.

[15] Y. D. Gamburg and G. Zangari, *Theory and Practice of Metal Electrodeposition*, Springer, New York, NY, USA, 2011.

[16] N. Guo, Q. Liu, Y. C. Xin, B. F. Luan, and Z. Zhou, "The application of back-scattered electron imaging for characterization of pearlitic steels," *Science China Technological Sciences*, vol. 54, no. 9, pp. 2368–2372, 2011.

[17] J. Zou, T. Grosdidier, K. Zhang, and C. Dong, "Mechanisms of nanostructure and metastable phase formations in the surface melted layers of a HCPEB-treated D2 steel," *Acta Materialia*, vol. 54, no. 20, pp. 5409–5419, 2006.

[18] J. J. Hu, G. B. Zhang, H. B. Xu, and Y. F. Chen, "Microstructure characteristics and properties of 40Cr steel treated by high current pulsed electron beam," *Materials Technology*, vol. 27, no. 4, pp. 300–303, 2012.

[19] J. Cheol Oh, D.-K. Choo, and S. Lee, "Microstructural modification and hardness improvement of titanium-base surface-alloyed materials fabricated by high-energy electron beam irradiation," *Surface and Coatings Technology*, vol. 127, no. 1, pp. 76–85, 2000.

[20] Z. Zhong and S. J. Clouser, "Nickel-tungsten alloy brush plating for engineering applications," *Surface and Coatings Technology*, vol. 240, pp. 380–386, 2014.